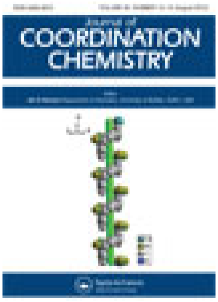

Journal of Coordination Chemistry
Publication details, including instructions for authors and subscription information:
http://www.tandfonline.com/loi/gcoo20

Syntheses, crystal structures, and optical properties of a series of transition metal coordination polymers with chelidamic acid and 4,4′-bipyridine

Jian-Ping Zou [a] [b] [c] , Shun-Chen Dai [a] , Wen-Ting Guan [a] , Hai-Bing Yang [a] , Ying-Feng Feng [a] & Xu-Biao Luo [a]

[a] Key Laboratory of Jiangxi Province for Ecological Diagnosis-Remediation and Pollution Control , Nanchang Hangkong University , Nanchang , Jiangxi 330063 , P.R. China

[b] Key Laboratory of Nondestructive Testing (Nanchang Hangkong University) , Ministry of Education , Nanchang , Jiangxi 330063 , P.R. China

[c] State Key Laboratory of Structural Chemistry , Fujian Institute of Research on the Structure of Matter, Chinese Academy of Sciences , Fuzhou , Fujian 350002 , P.R. China

To cite this article: Jian-Ping Zou , Shun-Chen Dai , Wen-Ting Guan , Hai-Bing Yang , Ying-Feng Feng & Xu-Biao Luo (2012) Syntheses, crystal structures, and optical properties of a series of transition metal coordination polymers with chelidamic acid and 4,4′-bipyridine, Journal of Coordination Chemistry, 65:16, 2877-2892, DOI: 10.1080/00958972.2012.705282

To link to this article: http://dx.doi.org/10.1080/00958972.2012.705282

Journal of Coordination Chemistry
Vol. 65, No. 16, 20 August 2012, 2877–2892

Syntheses, crystal structures, and optical properties of a series of transition metal coordination polymers with chelidamic acid and 4,4′-bipyridine

JIAN-PING ZOU*†‡§, SHUN-CHEN DAI†, WEN-TING GUAN†,
HAI-BING YANG†, YING-FENG FENG† and XU-BIAO LUO†

†Key Laboratory of Jiangxi Province for Ecological Diagnosis-Remediation and Pollution Control, Nanchang Hangkong University, Nanchang, Jiangxi 330063, P.R. China
‡Key Laboratory of Nondestructive Testing (Nanchang Hangkong University), Ministry of Education, Nanchang, Jiangxi 330063, P.R. China
§State Key Laboratory of Structural Chemistry, Fujian Institute of Research on the Structure of Matter, Chinese Academy of Sciences, Fuzhou, Fujian 350002, P.R. China

(*Received 29 February 2012; in final form 8 May 2012*)

A series of transition metal (Zn, Cu, Mn) complexes with chelidamic acid (2,6-dicarboxy-4-hydroxypyridine, H_3CAM) and 4,4′-bipyridine (bipy), $[Zn_2(bipy)Cl_2]_n$ (**1**), $\{[Zn_2(HCAM)(H_2CAM)_2]\cdot(bipy)\cdot 3.5H_2O\}_n$ (**2**), $[Mn_3(HCAM)_3(H_2O)_7]\cdot(bipy)\cdot 3H_2O$ (**3**), $[Mn_2(HCAM)_2(bipy)\cdot(H_2O)_2]\cdot 4H_2O$ (**4**), $[Cu_2(HCAM)_2(bipy)\cdot(H_2O)_2]\cdot 4H_2O$ (**5**), and $Cu_2(HCAM)_2(bipy)\cdot(H_2O)_2$ (**6**), have been synthesized by hydrothermal or solution methods and characterized by single-crystal X-ray diffraction. The structural analyses reveal that **1** exhibits a zigzag chain of Zn(II), Cl^-, and 4,4′-bipyridine. In **2**, a 1-D polymeric $[Zn_2(HCAM)(H_2CAM)_2]_n$ chain and a discrete 4,4′-bipyridine assemble into a 2-D supramolecular network *via* H-bonds. Complex **3** consists of asymmetric units of $Mn_3(HCAM)_3(H_2O)_7$ that are linked by hydrogen bonds to form a 2-D H-bonded network. Complexes **4**–**6** are isomorphous and possess discrete structures. The photoluminescent properties of **1**–**6** at room temperature were studied.

Keywords: Crystal structures; Coordination polymers; Photoluminescent properties; Chelidamic acid; 4,4′-Bipyridine

1. Introduction

Coordination polymers are an important interface between synthetic chemistry and materials science, providing a solid foundation for understanding how molecules organize and how functions can be achieved [1, 2]. A large number of complexes containing chelidamic acid have been reported, and they play a significant role in designing molecules and preparation of functional materials [3–8]. There are relatively fewer complexes built by chelidamic acid and bridging ligands such as 4,4′-bipyridine

---

*Corresponding author. Email: zjp_112@126.com

Journal of Coordination Chemistry
ISSN 0095-8972 print/ISSN 1029-0389 online
http://dx.doi.org/10.1080/00958972.2012.705282

are chosen for demonstrated ability to act as rods linking metal centers to give extended solids with diverse topologies [9]. To the best of our knowledge, 4,4′-bipyridine is rarely used in the syntheses of metal complexes with chelidamic acid [10–33]. To obtain metal complexes containing chelidamic acid and 4,4′-bipyridine, we reacted 4,4′-bipyridine and chelidamic acid with transition metal ions. Herein, we report syntheses, crystal structures, magnetic, and luminescent properties of a series of transition metal complexes with chelidamic acid and 4,4′-bipyridine, $[Zn_2(bipy)Cl_2]_n$ (**1**), $\{[Zn_2(HCAM)(H_2CAM)_2]\cdot(bipy)\cdot3.5H_2O\}_n$ (**2**), $[Mn_3(HCAM)_3(H_2O)_7]\cdot(bipy)\cdot3H_2O$ (**3**), $[Mn_2(HCAM)_2(bipy)\cdot(H_2O)_2]\cdot4H_2O$ (**4**), $[Cu_2(HCAM)_2(bipy)\cdot(H_2O)_2]\cdot4H_2O$ (**5**), and $Cu_2(HCAM)_2(bipy)\cdot(H_2O)_2$ (**6**).

2. Experimental

2.1. *Apparatus*

All chemicals were analytically pure (>99.99%) and used without purification. UV-Vis spectra were recorded at room temperature on a computer-controlled PE Lambda 900 UV-Vis spectrometer equipped with an integrating sphere from 200 to 2000 nm. Elemental analyses (C, H, and N) were carried out with an Elementar Vario EL. IR spectra were recorded on a Magna 750 FT-IR spectrometer as KBr pellets from 4000 to 400 cm^{-1}. Photoluminescence analyses were performed on an Edinburgh FLS920 fluorescence spectrometer. Thermogravimetry-differential thermal analyses (TG-DTA) were performed on a Perkin Elmer Diamond thermoanalyzer under N_2 from 25°C to 800°C at a heating rate of 10°C min^{-1}.

2.2. *Syntheses*

2.2.1. Synthesis of $[Zn_2(bipy)Cl_2]_n$ (1). Initially, a mixture of $Zn(Ac)_2\cdot2H_2O$ (0.02 mmol), $NdCl_3\cdot6H_2O$ (0.05 mmol), 4,4′-bipyridine (0.01 mmol), and chelidamic acid (0.1 mmol) was dissolved in 10 mL water and 5 mL DMF at pH = 7 to obtain a heterometal coordination polymer. Stirring for 4 h, filtering, and allowing to stand at room temperature over a period of 10 days gave yellow prismatic crystals of **1** that are stable in air. Yield: 20% (based on 4,4′-bipyridine). Anal. Calcd (%): C, 33.56; H, 2.25; N, 7.83. Found (%): C, 33.61; H, 2.30; N, 7.90. IR (KBr, cm^{-1}): 3433.04(s), 2924.21(vw), 1611.51(vs), 1536.98(w), 1489.63(w), 1416.70(s), 1214.48(w), 1116.01(vw), 1071.88(s), 1047.29(vw), 1015.37(w), 809.67(s), 727.15(w), 642.93(s), 497.02(w).

2.2.2. Synthesis of $\{[Zn_2(HCAM)(H_2CAM)_2]\cdot(bipy)\cdot3.5H_2O\}_n$ (2). $Zn(Ac)_2\cdot2H_2O$ (0.06 mmol), 4,4′-bipyridine (0.05 mmol), and chelidamic acid (0.1 mmol) were dissolved in 10 mL water at pH = 6. Yellow prism-shaped crystals of **2** were obtained over 7 days. Yield: 33% (based on chelidamic acid). Anal. Calcd (%): C, 40.48; H, 3.18; N, 7.62. Found (%): C, 40.50; H, 3.31; N, 7.66. IR (KBr, cm^{-1}): 3417.91(s), 3103.85(s), 2728.01(w), 1644.46(w), 1493.77(w), 1415.86(w), 1266.81(s), 1208.45(vw), 1121.34(s), 1052.20(s), 932.53(w), 891.88(w), 810.62(s), 743.39(s), 641.16(w), 583.78(w), 501.58(vw).

2.2.3. Synthesis of [$Mn_3(HCAM)_3 \cdot (H_2O)_7$] • (bipy) • $3H_2O$ (3). The process of synthesis is the same as that of **1** except for reactant (for **3**: $MnSO_4 \cdot H_2O$ (0.1 mmol), 4,4′-bipyridine (0.1 mmol), and chelidamic acid (0.1 mmol)). Light yellow prismatic crystals of **3** that are stable in air were obtained by filtration of the resulting solution. Yield: 78% (based on chelidamic acid). Anal. Calcd (%): C, 35.65; H, 3.57; N, 6.71. Found (%): C, 35.68; H, 3.59; N, 6.75. IR (KBr, cm^{-1}): 3853.93(vw), 3747.19(vw), 3362.80(vs), 2731.89(vw), 2628.60(w), 2499.85(vw), 1599.95(w), 1572.30(vs), 1413.14(vs), 1337.36(w), 1119.66(w), 1069.12(w), 1028.15(s), 942.46(vw), 896.15(vw), 808.82(s), 743.86(w), 623.52(w), 587.82(w), 501.04(vw).

2.2.4. Synthesis of [$Mn_2(HCAM)_2(bipy) \cdot (H_2O)_2$] • $4H_2O$ (4). A mixture of $MnSO_4 \cdot H_2O$ (0.07 mmol), 4,4′-bipyridine (0.05 mmol), chelidamic acid (0.1 mmol), and water (10 mL) was loaded into a 25-mL Teflon-lined autoclave and heated at 413 K for 2 days. Then the solution was cooled to room temperature over 3 days. Yellow prismatic crystals of **4** that are stable in air were obtained by filtration of the resulting solution. Yield: 71% (based on chelidamic acid). Anal. Calcd (%): C, 39.13; H, 3.56; N, 7.61. Found (%): C, 39.15; H, 3.59; N, 7.63. IR (KBr, cm^{-1}): 3521.38(vw), 3390.88(s), 1651.75(vw), 1645.21(vw), 1621.73(w), 1502.19(w), 1462.16(w), 1403.25(vs), 1331.69(vs), 1231.67(s), 1120.25(w), 1081.69(w), 1054.76(vs), 970.11(vw), 935.02(w), 884.77(w), 809.77(vs), 750.70(w), 651.13(w), 580.11(w), 504.09(w).

2.2.5. Synthesis of [$Cu_2(HCAM)_2(bipy) \cdot (H_2O)_2$] • $4H_2O$ (5). The process of synthesis is same to that of **1** except for reactant (for **5**: $Cu(CH_3COO)_2 \cdot H_2O$ (0.08 mmol), $La(CH_3COO)_3 \cdot 6H_2O$ (0.1 mmol), 4,4′-bipyridine (0.1 mmol), and chelidamic acid (0.1 mmol)). The initial purpose was to synthesize a heterometal coordination polymer, but only blue prismatic crystals of **5** that are stable in air were obtained over a period of 4 days. Yield: 76% (based on chelidamic acid). Anal. Calcd (%): C, 38.30; H, 3.48; N, 7.45. Found (%): C, 38.34; H, 3.50; N, 7.49. IR (KBr, cm^{-1}): 3392.71(w), 3054.28(w), 2729.13(vw), 2612.58(vw), 2505.18(vw), 1633.56(s), 1487.08(w), 1464.36(w), 1369.57(vs), 1308.39(vw), 1258.46(w), 1214.26(w), 1070.24(s), 925.25(w), 863.89(w), 805.38(s), 746.85(w), 655.02(w), 575.92(w), 503.69(vw).

2.2.6. Synthesis of $Cu_2(HCAM)_2(bipy) \cdot (H_2O)_2$ (6). A mixture of $Cu(CH_3COO)_2 \cdot H_2O$ (0.1 mmol), chelidamic acid (0.1 mmol), 4,4′-bipyridine (0.1 mmol), and water (10 mL) was loaded into a 25-mL Teflon-lined autoclave, heated at 433 K for 2d, after which it was cooled to room temperature over 3 days. Blue prismatic crystals of **6** that are stable in air were obtained by filtration of the resulting solution. Yield: 60% (based on chelidamic acid). Anal. Calcd (%): C, 44.73; H, 2.19; N, 8.71. Found (%): C, 44.76; H, 2.21; N, 8.75. IR (KBr, cm^{-1}): 3054.50(vw), 2730.66(vw), 2613.57(vw), 2506.04(vw), 1826.86(vw), 1634.03(vs), 1534.11(vw), 1487.10(vw), 1464.92(w), 1366.34(s), 1308.49 (w), 1259.33(w), 1215.06(w), 1113.89(w), 1070.57(s), 971.95(w), 919.48(w), 864.92(w), 807.69(w), 747.53(w), 724.99(w), 656.28(w), 640.31(w), 576.11(w), 503.93(w), 438.61(s).

2.3. *Single-crystal X-ray structure determination*

Single crystals of **1**–**6** suitable for X-ray analyses were mounted, respectively, at the apex of a glass fiber for X-ray diffraction data collection. Data sets of **1**, **4**, and **6** were collected on a SMART APEX CCD diffractometer and those of **2**, **3**, and **5** were collected on Rigaku Mercury CCD using graphite monochromated Mo-Kα radiation ($\lambda = 0.71073$ Å) from a rotating anode generator at 293 K. The intensity data were collected with an ω scan technique and corrected for *Lorentz-polarization* factors. All structures were solved by direct methods and refined on F^2 with full-matrix least-squares using Siemens SHELXTL™ version 5 package of crystallographic software [34]. The final refinements included anisotropic displacement parameters for all non-hydrogen atoms and a secondary extinction correction. Hydrogen atoms of coordinated water for **3**–**6** and uncoordinated water for **5** and those of hydroxyl oxygen for **2**–**6** were found in the difference Fourier map and refined with the distance restraints of 0.79–0.85 Å for O–H bonds and in riding mode with $U_{\text{iso}}(\text{H})$ values of $1.5U_{\text{eq}}(\text{O})$. Hydrogen atoms of uncoordinated water for **2**, **3**, **4**, and **6** are not included. Other hydrogen atoms were allowed to ride on their respective parent with the distance restraint of 0.93 Å for C–H bonds and were included in the refinement with isotropic displacement parameters $U_{\text{iso}}(\text{H}) = 1.2U_{\text{eq}}(\text{C})$. Crystallographic data of **1**–**6** are listed in table 1. Selected bond lengths are given in table 2. Hydrogen bonds of **2**–**6** are listed in table 3.

2.4. *Computational descriptions*

Crystallographic data of **1** determined by X-ray were used to calculate the electronic band structure. Calculation of the electronic band structure along with density of states (DOSs) was carried out with density functional theory using one of the three nonlocal gradient corrected exchange-correlation functional and performed with the CASTEP code [35], which uses a plane wave basis set for the valence electrons and norm-conserving pseudopotential for the core electrons [36]. The number of plane waves included in the basis was determined by a cutoff energy E_c of 700 eV. Pseudoatomic calculations were performed for H-1s^1, C-2s^{2}2p^2, N-2s^{2}2p^3, Cl-3s^{2}3p^5, and Zn-3d^{10}4s^2. The parameters used in the calculations and convergence criteria were set by default values of the CASTEP code [37]. Calculations of linear optical properties were also accomplished. CASTEP calculated the real $\varepsilon_1(\omega)$ and imaginary $\varepsilon_2(\omega)$ parts of the dielectric function. The $\varepsilon_2(\omega)$ can be thought of as detailing the real transitions between occupied and unoccupied electronic states. The real and imaginary parts were linked by a Kramers–Kronig transform [38]. This transform was used to obtain the real part $\varepsilon_1(\omega)$ of the dielectric function.

3. Results and discussion

3.1. *Crystal structure of 1*

As shown in figure 1(a), the asymmetric unit of **1** consists of one Zn(II), one 4,4′-bipyridine, and two coordinated chlorides. In **1**, the Zn(II) centers are bridged

Table 1. Crystal data and structure refinement of **1**–6.

Complex	**1**	**2**	**3**	**4**	**5**	**6**
Empirical formula	$C_{10}H_8ZnCl_2N_2$	$C_{31}H_{24}Zn_2N_5O_{18.50}$	$C_{31}H_{37}Mn_3N_5O_{25}$	$C_{24}H_{13}Mn_2N_4O_{16}$	$C_{24}H_{26}Cu_2N_4O_{16}$	$C_{24}H_{18}Cu_2N_4O_{12}$
Formula weight	292.45	893.29	1044.48	723.26	753.57	681.50
Crystal system	Monoclinic	Monoclinic	Monoclinic	Orthorhombic	Orthorhombic	Monoclinic
Space group	*C*2/*c*	*P*2$_1$/*c*	*P*2$_1$/*c*	*Pbca*	*Pbca*	*P*2$_1$/*c*
Unit cell dimensions (Å, °)						
a	15.860(5)	10.144(4)	7.4891(8)	19.8777(9)	19.920(7)	8.3980(4)
b	5.1198(14)	20.317(8)	30.021(3)	7.0297(3)	7.041(3)	18.4486(8)
c	14.613(5)	18.900(6)	18.345(2)	20.2275(10)	20.241(7)	7.8681(3)
α	90	90	90	90	90	90
β	110.286(6)	111.560(17)	96.6830(10)	90	90	100.040
γ	90	90	90	90	90	90
Volume (Å^3), *Z*	1113.0(6), 4	3623(2), 4	4096.5(8), 4	2826.5(2), 4	2838.7(18), 4	1200.35(9), 2
Crystal size (mm^3)	0.24 × 0.15 × 0.10	0.20 × 0.20 × 0.20	0.35 × 0.30 × 0.20	0.30 × 0.25 × 0.20	0.30 × 0.25 × 0.20	0.33 × 0.23 × 0.20
Absorption coefficient (mm^{-1})	2.651	1.412	1.011	0.980	1.585	1.852
Calculated density (g cm^{-3})	1.745	1.638	1.694	1.7000	1.763	1.886
F(000)	584	1812	2132	1452	1536	688
θ range (°)	2.74–25.24	2.32–25.25	2.32–25.50	2.26–25.50	2.26–27.47	2.46–25.25
Reflections collected/unique	3784/999; $R_{\text{int}} = 0.0311$	23,368/6562; $R_{\text{int}} = 0.0396$	23,789/7573; $R_{\text{int}} = 0.0170$	20,231/2628; $R_{\text{int}} = 0.0316$	20,325/3243; $R_{\text{int}} = 0.0276$	8890/2165; $R_{\text{int}} = 0.0213$
Goodness of fit on F^2	0.994	1.010	1.000	1.002	1.017	1.006
R_1^{a}, wR_2^{b} $[I > 2\sigma(I)]$	0.0504, 0.1388	0.0446, 0.1388	0.0446, 0.1388	0.0350, 0.1075	0.0413, 0.1279	0.0269, 0.0873
R_1, wR_2 (all data)	0.0567, 0.1491	0.0446, 0.1388	0.0350, 0.1075	0.0602, 0.2101	0.0413, 0.1279	0.0269, 0.0873

[a] $R_1 = \sum||F_o| - |F_c||/\sum|F_o|$; [b] $wR_2 = \{\sum[w(F_o^2 - F_c^2)^2]/\sum[w(F_o^2)^2]\}^{1/2}$.

Table 2. Selected bond lengths (Å) of **1**–**6**.

1			
Zn(1)–N(1)	2.061(3)	Zn(1)–Cl(1) × 2	2.2157(13)
2			
Zn(1)–N(5)	2.005(2)	Zn(2)–O(34)	1.995(2)
Zn(1)–N(4)	2.012(2)	Zn(2)–N(3)	1.999(2)
Zn(1)–O(24)	2.107(2)	Zn(2)–O(11)	2.177(2)
Zn(1)–O(33)	2.159(2)	Zn(2)–O(13)	2.179(2)
Zn(1)–O(31)	2.301(2)	Zn(2)–O(32)	1.945(2)
Zn(1)–O(21)	2.309(2)		
3			
Mn(1)–O(6)	2.1440(14)	Mn(2)–O(4)	2.3254(13)
Mn(1)–N(3)	2.1460(16)	Mn(2)–O(6)	2.3732(14)
Mn(1)–O(4W)	2.1542(17)	Mn(2)–O(8)	2.4650(14)
Mn(1)–O(3W)	2.1809(16)	Mn(3)–O(1W)	2.1430(15)
Mn(1)–O(1)	2.2590(15)	Mn(3)–O(2W)	2.1838(16)
Mn(1)–O(4)	2.2878(13)	Mn(3)–N(5)	2.2073(16)
Mn(2)–O(5W)	2.1506(15)	Mn(3)–O(13)	2.2853(14)
Mn(2)–O(6W)	2.1694(16)	Mn(3)–O(8)	2.2883(14)
Mn(2)–O(7W)	2.1965(15)	Mn(3)–O(12)	2.3065(14)
Mn(2)–N(4)	2.2868(16)		
4			
Mn(1)–O(1W)	1.983(4)	Mn(1)–O(5)	2.215(3)
Mn(1)–N(2)	1.994(3)	Mn(1)–O(1)	2.167(3)
Mn(1)–N(1)	1.998(3)		
5			
Cu(1)–O(3W)	1.978(2)	Cu(1)–O(2)	2.1717(16)
Cu(1)–N(1)	1.9913(16)	Cu(1)–O(3)	2.2260(16)
Cu(1)–N(2)	1.9956(18)		
6			
Cu(1)–N(1)	1.8917(15)	Cu(1)–O(1)	2.0076(13)
Cu(1)–N(2)	1.9493(15)	Cu(1)–O(1W)	2.3953(14)
Cu(1)–O(3)	2.0030(13)		

by 4,4′-bipyridine and two coordinated Cl^- to form a slightly distorted tetrahedron (figure 1a) [39]. The Zn–N bond distance is 2.061(3) Å and the Zn–Cl bond distance is 2.2157(13) Å (table 2). Similar to structures of Cu, Ni, Co, and Fe complexes reported in the literature [39–41], Zn in **1** is interconnected through the 4,4′-bipyridine to generate a 1-D architecture (figure 1b).

3.2. *Crystal structure of 2*

Complex **2** consists of two Zn(II) ions, three chelidamic acid ligands, three and a half uncoordinated water molecules, and one discrete 4,4′-bipyridine (figure 2a). The asymmetric unit of the compound has two crystallographically Zn's with different coordination types; Zn(1) is six-coordinate by four oxygen atoms and two nitrogen atoms from two different chelated chelidamic acid ligands in a distorted octahedral geometry, while Zn(2) is five-coordinate by two oxygen atoms and one nitrogen atom from one chelated chelidamic acid ligand, and two carboxylate oxygen atoms from the

Table 3. Hydrogen bonds of **2**–**6**.

D–H···A	d(D–H) (Å)	d(H···A) (Å)	d(D···A) (Å)	∠(DHA) (°)
2				
O(15)–H(15B)···O(22)$^{\mathrm{i}}$	0.82	1.82	2.638(3)	172.9
O(25)–H(25B)···O(5WB)	0.82	1.73	2.547(13)	170.6
O(25)–H(25B)···O(5WA)	0.82	1.97	2.670(5)	143.3
O(35)–H(35B)···O(21)$^{\mathrm{ii}}$	0.82	1.79	2.598(3)	170.5
3				
O(1W)–H(1WB)···O(7)$^{\mathrm{i}}$	0.830(10)	1.903(14)	2.683(2)	156(3)
O(2W)–H(2WB)···O(7)$^{\mathrm{ii}}$	0.843(10)	1.939(11)	2.771(2)	169(3)
O(6W)–H(6WA)···O(10W)$^{\mathrm{ii}}$	0.857(10)	1.912(11)	2.754(2)	167(3)
O(3W)–H(3WA)···O(13)$^{\mathrm{iii}}$	0.849(10)	1.947(14)	2.757(2)	159(3)
O(4W)–H(4WB)···O(9)$^{\mathrm{iv}}$	0.867(10)	1.933(16)	2.756(2)	158(3)
O(7W)–H(7WA)···O(14)$^{\mathrm{iv}}$	0.837(10)	1.986(13)	2.777(2)	157(2)
O(7W)–H(7WB)···O(9W)$^{\mathrm{iv}}$	0.845(10)	1.987(10)	2.825(2)	172(3)
O(5)–H(5A)···O(11)$^{\mathrm{v}}$	0.82	1.72	2.541(2)	177.6
O(10)–H(10A)···N(1)$^{\mathrm{vi}}$	0.82	1.92	2.734(3)	169.0
O(15)–H(15B)···O(2)$^{\mathrm{vii}}$	0.82	1.77	2.582(2)	173.4
O(2W)–H(2WA)···O(6W)	0.848(10)	2.153(10)	2.997(2)	174(3)
O(4W)–H(4WA)···O(7W)	0.848(10)	2.176(17)	2.923(2)	147(3)
O(5W)–H(5WA)···O(12)	0.837(10)	1.870(10)	2.704(2)	174(3)
O(5W)–H(5WB)···O(3)	0.844(10)	1.857(15)	2.623(2)	150(3)
O(6W)–H(6WB)···O(8W)	0.843(10)	1.807(10)	2.649(2)	178(3)
4				
O(1W)–H(1WA)···O(2)$^{\mathrm{i}}$	0.86(2)	1.83(3)	2.640(4)	156(6)
O(3)–H(3B)···O(2W)$^{\mathrm{ii}}$	0.82	1.79	2.609(5)	177.5
O(1W)–H(1WB)···O(5)$^{\mathrm{iii}}$	0.85(2)	1.92(4)	2.669(4)	146(6)
5				
O(1W)–H(1WA)···O(2)$^{\mathrm{i}}$	0.860(18)	1.91(2)	2.757(2)	166(3)
O(1W)–H(1WB)···O(2W)$^{\mathrm{i}}$	0.844(18)	2.031(19)	2.867(3)	171(4)
O(2W)–H(2WA)···O(1)$^{\mathrm{ii}}$	0.854(18)	2.06(2)	2.850(3)	154(3)
O(2W)–H(2WB)···O(1)$^{\mathrm{iii}}$	0.838(18)	2.161(19)	2.993(3)	172(4)
O(3W)–H(3WA)···O(3)$^{\mathrm{ii}}$	0.825(18)	1.858(19)	2.667(2)	167(3)
O(3W)–H(3WB)···O(4)$^{\mathrm{iv}}$	0.855(17)	1.808(18)	2.659(3)	173(4)
O(5)–H(5B)···O(1W)	0.82	1.78	2.595(3)	176.8
6				
O(1W)–H(1WA)···O(2)$^{\mathrm{i}}$	0.767(19)	2.21(2)	2.9475(19)	160(3)
O(1W)–H(1WA)···O(1)$^{\mathrm{i}}$	0.767(19)	2.55(2)	3.1947(18)	143(2)
O(1W)–H(1WB)···O(4)$^{\mathrm{ii}}$	0.80(2)	1.92(2)	2.6828(19)	160(3)
O(5)–H(5A)···O(1W)$^{\mathrm{iii}}$	0.82	1.86	2.6737(19)	169.5

Symmetry transformations used to generate equivalent atoms: For **2**: $^{\mathrm{i}}x-1, -y-1/2, z-1/2$; $^{\mathrm{ii}}-x+3, -y, -z-2$. For **3**: $^{\mathrm{i}}x+1, -y+3/2, z+1/2$; $^{\mathrm{ii}}x, -y+3/2, z+1/2$; $^{\mathrm{iii}}x-1, -y+3/2, z-1/2$; $^{\mathrm{iv}}x, -y+3/2, z-1/2$; $^{\mathrm{v}}-x+1, -y+1, -z+1$; $^{\mathrm{vi}}-x+1, -y+2, -z+1$; $^{\mathrm{vii}}x+1, y, z+1$. For **4**: $^{\mathrm{i}}-x+1/2, y-1/2, z$; $^{\mathrm{ii}}x, -y+3/2, z-1/2$; $^{\mathrm{iii}}-x, y-1/2, -z+1/2$. For **5**: $^{\mathrm{i}}x, -y+3/2, z+1/2$; $^{\mathrm{ii}}-x, y-1/2, -z+1/2$; $^{\mathrm{iii}}x, -y+3/2, z-1/2$; $^{\mathrm{iv}}-x+1/2, y-1/2, z$. For **6**: $^{\mathrm{i}}x, -y+1/2, z+1/2$; $^{\mathrm{ii}}-x+1, -y+1, -z+1$; $^{\mathrm{iii}}x-1, y, z$.

neighboring chelidamic acid to form a distorted trigonal-bipyramidal geometry. Zn–O and Zn–N bond distances range from 1.945(2) to 2.309(2) Å and 1.999(2) to 2.012(2) Å (table 2), respectively, which all lie in the normal range of reported Zn complexes with chelidamic acid [42–45]. The asymmetric units of $Zn_2(HCAM)(H_2CAM)_2$, comprised by two coordination polyhedra, are linked through carboxylate oxygen (O(34)) to form a 1-D chain along the *a*-axis and bridged through hydrogen bonds between the O(15) and O(22) (O(15)···O(22) = 2.638(3) Å) to form a 2-D network (figure 2b and c).

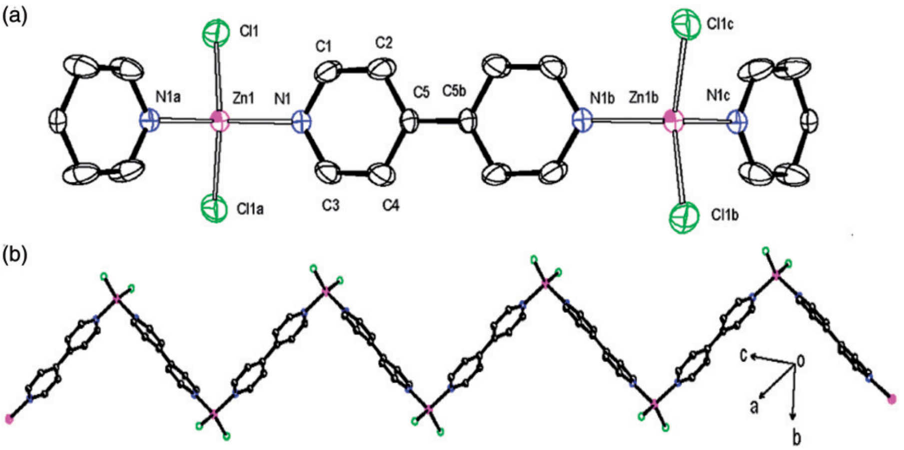

Figure 1. (a) View of the coordination unit of **1** with 30% probability of thermal ellipsoids. Hydrogen atoms are omitted for clarity. Symmetry codes for a: $-x$, y, $-1/2-z$; b: $1/2-x$, $1/2-y$, $-z$; c: $1/2+x$, $1/2-y$, $1/2+z$. (b) View of the 1-D zigzag chain of **1** along the *b*-axis.

The 2-D network is further linked by hydrogen bonds between water molecules and carboxylate or hydroxyl to form a 3-D supramolecular framework.

3.3. *Crystal structure of 3*

Single-crystal X-ray analysis reveals that there are three chelidamic acid ligands, one discrete 4,4′-bipyridine, and three crystallographically independent Mn(II) ions with different coordination environments in **3**. Mn(1) and Mn(3) are six-coordinate with distorted octahedral geometry with two oxygen atoms and one nitrogen atom from one chelated tridentate chelidamic acid ligand, one oxygen atom from neighboring chelated chelidamic acid, and two coordinated water molecules. Mn(2) is seven-coordinate with distorted pentagonal-bipyramidal geometry, where equatorial coordination consists of two oxygen atoms and one nitrogen atom from chelated chelidamic acid, one carboxylate oxygen atom from neighboring chelidamic acid, and one coordinated water molecule, while the axial positions are occupied by two coordinated water molecules (figure 3a). Mn–O bond distances range from 2.1430(15) to 2.4650(14) Å and Mn–N bond distances range from 2.1460(16) to 2.2868(16) Å (table 2), respectively, in the normal range of reported Mn complexes with chelidamic acid [21, 22]. The asymmetric units of $Mn_3(HCAM)_3(H_2O)_7$ are linked by hydrogen bonds involving water and carboxylate to form a 2-D layer (figure 3b). These layers are inter-linked through a very complex hydrogen-bonding network involving water and oxygen atoms from chelidamic acid ligands to form a 3-D supramolecular network.

3.4. *Crystal structures of 4–6*

Single-crystal X-ray diffraction analyses reveal that **4** and **5** are isomorphous, so we only choose **4** for detailed structural discussion. As shown in figure 4(a), the asymmetric unit of **4** consists of one Mn(II), one chelidamic acid ligand, one coordinated water

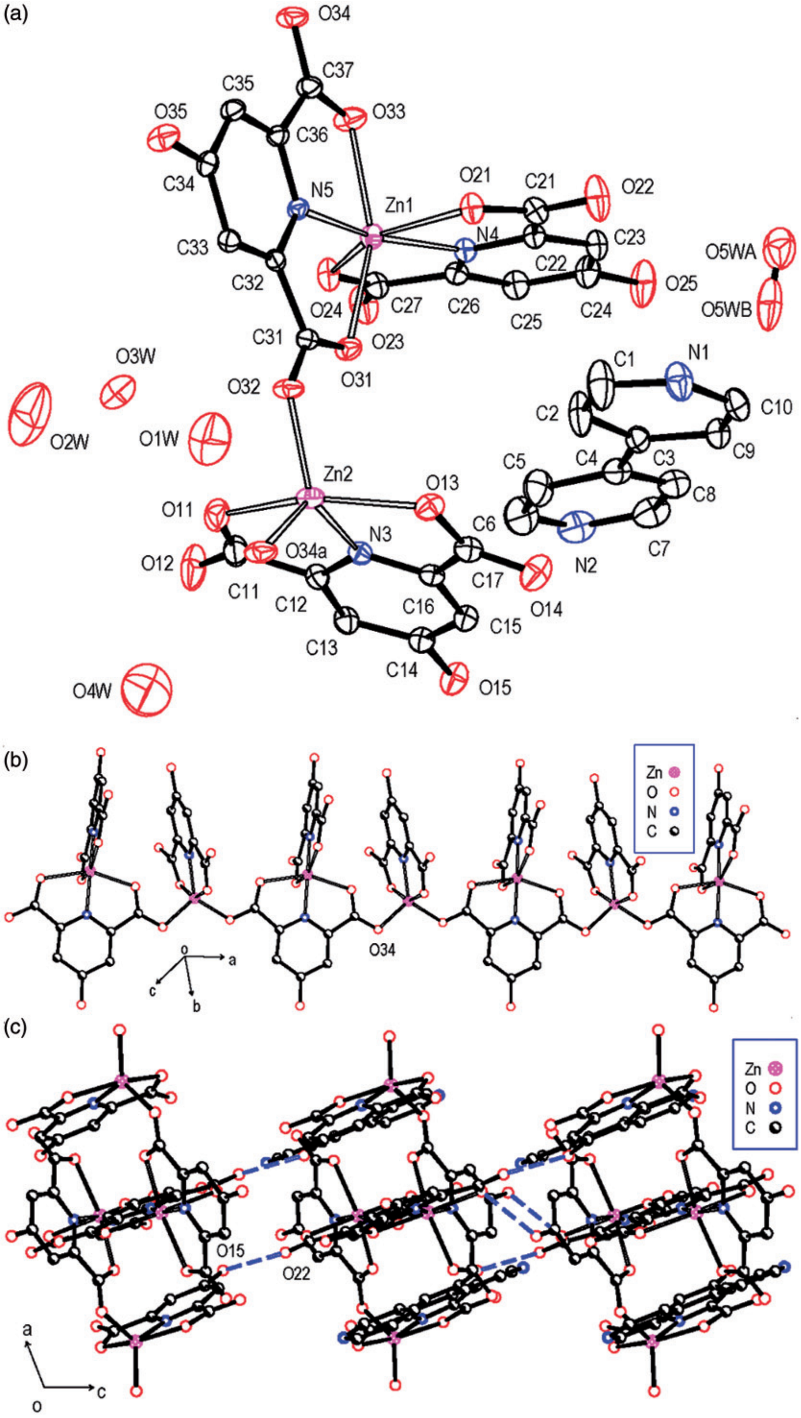

Figure 2. (a) View of the coordination unit of **2** with 30% probability of thermal ellipsoids. Hydrogen atoms are omitted for clarity. Symmetry codes for a: $-1+x$, y, z. (b) View of the 1-D chain of **2** along the *c*-axis. (c) View of the 2-D network built from polyhedra of **2** along the *b*-axis. Hydrogen atoms and uncoordinated atoms of pyridine rings and hydroxyl groups are omitted.

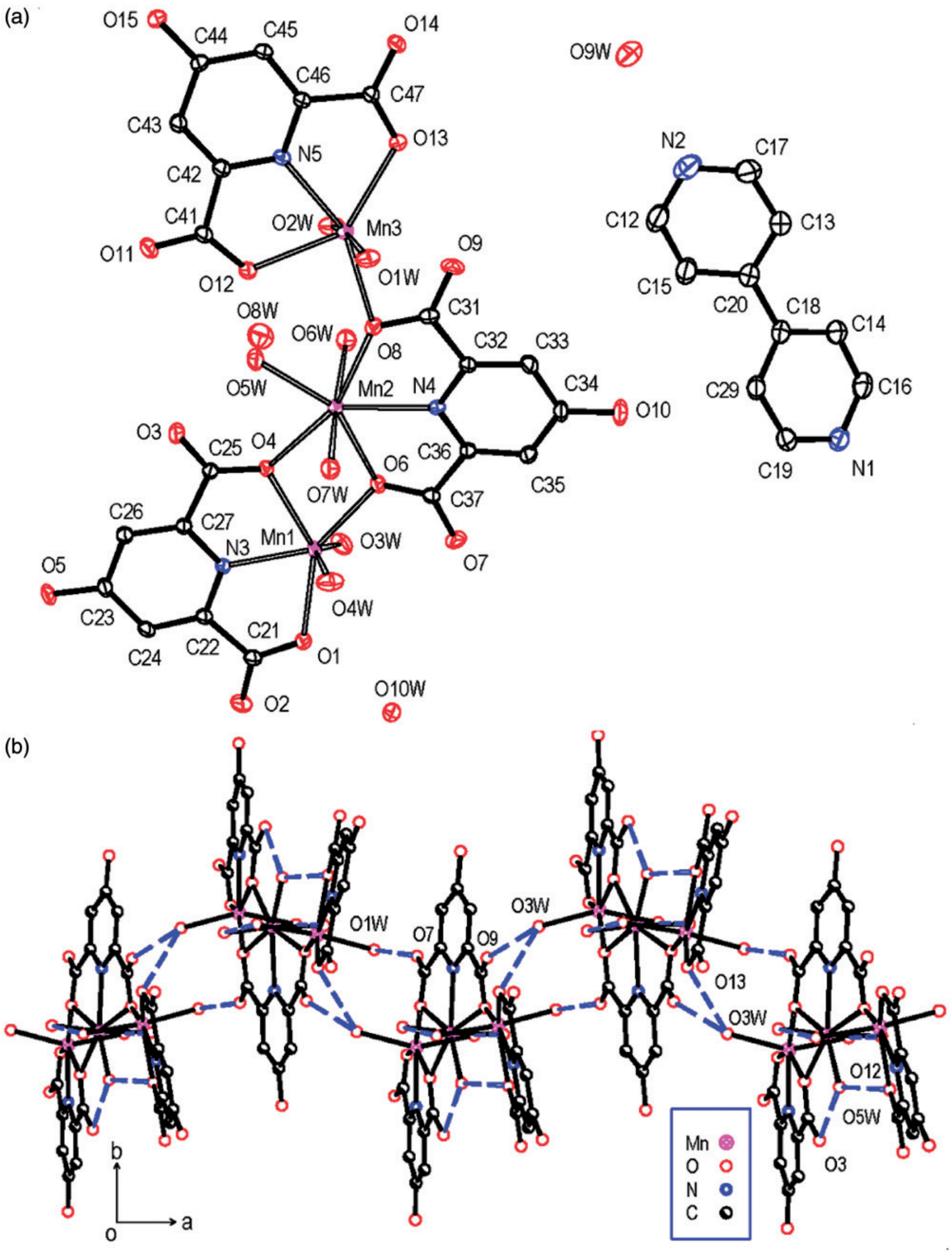

Figure 3. (a) View of the coordination unit of **3** with 30% probability of thermal ellipsoids. Hydrogen atoms are omitted for clarity. (b) View of the 2-D network of **3** along the *c*-axis.

molecule, one bridged 4,4′-bipyridine ligand, and two discrete water molecules. Mn(II) exhibits five-coordination with a distorted trigonal-bipyramid made up of two oxygen atoms and one nitrogen atom from chelated chelidamic acid, one nitrogen atom from bridging 4,4′-bipyridine, and one coordinated water molecule (figure 4a). The Mn–O

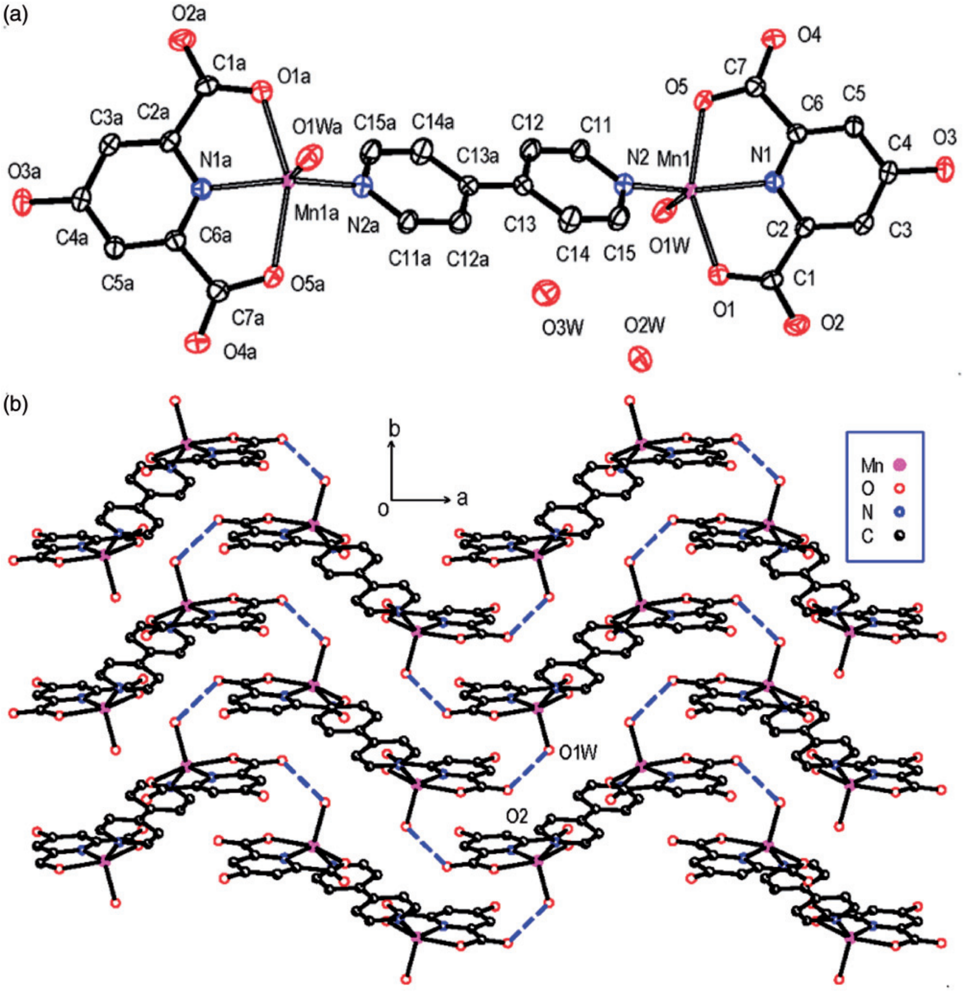

Figure 4. (a) View of the coordination unit of **4** with 30% probability of thermal ellipsoids. Hydrogen atoms are omitted for clarity. Symmetry codes for a: $-x$, $2-y$, $1-z$. (b) View of the 2-D network of **4** along the *c*-axis.

bond distances range from 1.983(4) to 2.215(3) Å and the M–N bond distance is 1.998(3) Å (table 2), in the normal range of reported Mn complexes with chelidamic acid [46, 47]. The asymmetric units of $Mn(HCAM)(H_2O)$ are linked by hydrogen bonds involving water and carboxylate, extending the structure into a 2-D layer (figure 4b). Hydrogen bonds between carboxylate oxygen atoms, hydroxyl oxygen atoms, and discrete water molecules link the 2-D coordination network to form a 3-D supramolecular structure. As for **6**, its structure is very similar to that of **4** except for a different space group (*Pbca* for **4** and $P2_1/c$ for **6**) and the different geometrical configuration of Cu ions. The geometry around Cu(II) is distorted trigonal-bipyramidal for **4**, but distorted square-pyramidal for **6** (figure 4a and figure S1). Herein structural detail of **6** is not discussed.

In addition, compared with other metal complexes with chelidamic acid or pyridine-2,6-dicarboxylic acid recently reported in the literature [23, 28, 32, 48], the present complexes **2**–**6** have different structural features and all contain the auxiliary 4,4′-bipyridine. The 4,4′-bipyridine coordinates to metal in **4**–**6**, whereas the auxiliary ligand does not coordinate to the metal ions among the reported complexes with chelidamic acid or pyridine-2,6-dicarboxylic acid [23, 28, 32, 48]. Therefore, we can conclude that the auxiliary ligands, such as 4,4′-bipyridine, 2,2′-bipyridine, 1,10-phenanthroline, and DMF, can affect the structures of the complexes based on the above structural comparisons.

3.5. *Luminescent properties*

Solid-state electronic emission spectra of **1**–**6** at room temperature show luminescence features (figure 5). Complex **1** shows fluorescence with maximum emission at 352 nm upon excitation at 300 nm and **2** displays yellow fluorescence with the maximum emission at 564 nm upon excitation at 359 nm. Complexes **3**, **5**, and **6** all display blue fluorescence with maximum emission at 467 nm, 483 nm, and 438 nm upon excitation at 372 nm, 394 nm, and 380 nm. Complex **4** displays green fluorescence with maximum emission at 525 nm upon excitation at 398 nm. The strongest emission peaks for free chelidamic acid and 4,4′-bipyridine are 525 nm and 385 nm, respectively, both due to $\pi \rightarrow \pi^*$ transition [16, 49]. Compared to the free 4,4′-bipyridine, **1** exhibits a blue shift of 33 nm. Compared to free chelidamic acid, **3**, **5**, and **6** result in a blue shift of 57 nm, 42 nm, and 87 nm, respectively, whereas **2** results in a red shift of 39 nm. The results indicate that the emission of **1** may originate from π–π^* transition of 4,4′-bipyridine and the emissions of **3**–**6** may be all attributed to the π–π^* transition of chelidamic acid, while the emission of **2** may originate from charge transition between chelidamic acid and metal ions [49].

3.6. *IR spectra*

As shown in figure S2, IR spectra of **2**–**6** show broad peaks at 3600–3100 cm^{-1} due to hydrogen-bonding between water molecules. The ν(C=O) of chelidamic acid is at 1730 cm^{-1}. This strong band disappears after coordination, which indicates coordination *via* carboxylic oxygen in **2**–**6**. The IR attributions are consistent with the structural determinations.

3.7. *TGA analysis*

To investigate the stability of **3**, thermogravimetric analysis (TGA) was carried out on **3**. As shown in figure S3, TG/DTA curves show that **3** undergoes a three-step decomposition between 25°C and 800°C. The first weight loss of 17.10% (Calcd 17.24%) is completed at about 200°C, corresponding to loss of 10 water molecules (three discrete and seven coordinated water molecules) per formula unit. The second weight loss of 16.81% (Calcd 18.06%) at 200–430°C is from loss of the discrete 4,4′-bipyridine. From 400°C to 800°C weight loss of 24.15% (Calcd 25.56%)

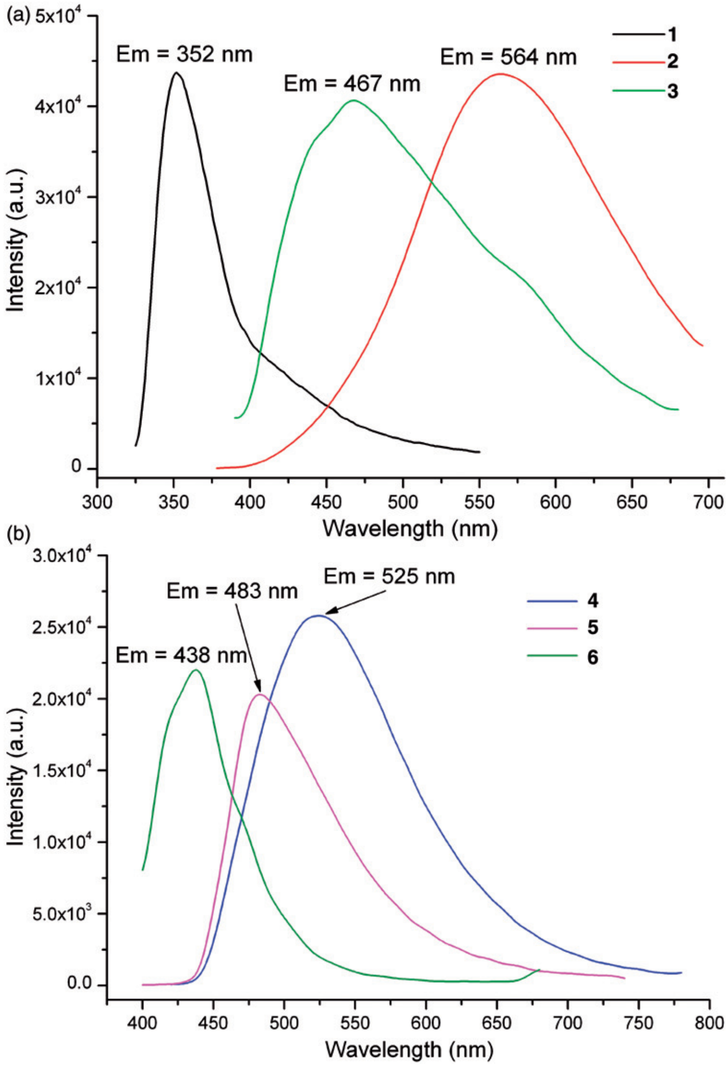

Figure 5. Solid-state emission spectra of **1**–**6** ((a) for **1**–**3** and (b) for **4**–**6**, respectively).

corresponds to loss of one chelidamic acid ligand. These results are consistent with the X-ray crystal structure.

3.8. *Band structure and DOS of 1*

The calculated band structure of **1** along high symmetry points of the first Brillouin zone is plotted in figure 6. The top of valence bands (VBs) and the bottom of conduction bands (CBs) are both relatively flat. The highest energy (0.00 eV) of VBs and the lowest energy (2.88 eV) of CBs in **1** are both localized at the Z point. According to the calculation, the solid **1** thus possesses a direct energy band gap of 2.88 eV, which

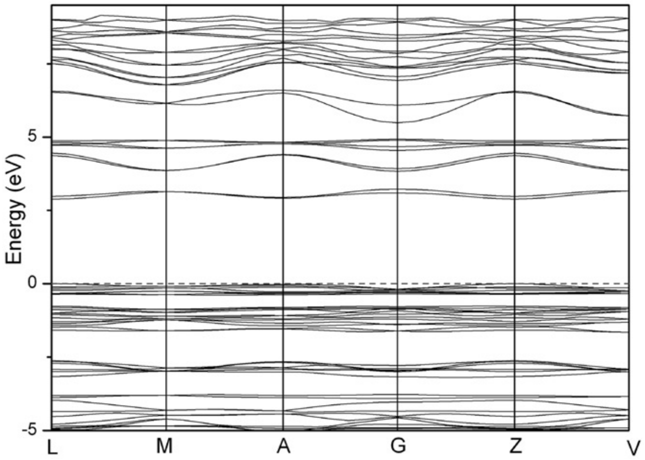

Figure 6. Energy band structures of **1**. Energy bands are shown only between −4.0 and 4.1 eV for clarity, and the Fermi level is set at 0 eV.

is close to its experimental value (3.55 eV) shown in figure S4. The bands can be assigned according to total and partial DOSs, as plotted in figure 7. The VBs between −20.0 and −5.0 eV are mostly formed by Zn-3d, C-2s, C-2p, and Cl-3s states, mixing with small N-2s and N-2p states. VBs between −5.0 eV and the Fermi level (0.0 eV) are mainly contribution from C-2p and Cl-3p states mixing with a small amount of N-2p state, while the CBs between 2.5 and 10.0 eV are contribution from C-2p and N-2p states mixing with a small amount of Zn-4s state.

From dispersion of the calculated $\varepsilon_2(\omega)$ spectra, the calculated strongest absorption peak (also first absorption peak) localizes at 4.11 eV (302 nm) with polycrystalline geometry (figure S5), which is close to the strongest photo-excitation at 300 nm. Accordingly, the origin of the emission band may be mainly ascribed to intra-ligand charge transfer, where the charges are transferred between the C-2p and C-2p states [16, 19]. This analysis is consistent with the above experimental result.

4. Conclusion

Six complexes with chelidamic acid and 4,4′-bipyridine have been synthesized and structurally characterized by X-ray single-crystal diffraction. The structure of **1** exhibits a zigzag chain, **2** contains a 1-D polymeric $[Zn_2(HCAM)(H_2CAM)_2]_n$ chain and a discrete 4,4′-bipyridine, and then further assemble into 2-D supramolecular networks *via* H-bonds. Complex **3** consists of asymmetric units of $Mn_3(HCAM)_3(H_2O)_7$ that are linked by hydrogen bonds to form a 2-D H-bonded network. Complexes **4–6** are isomorphous and possess discrete structures. Complexes **1–6** exhibit good luminescence.

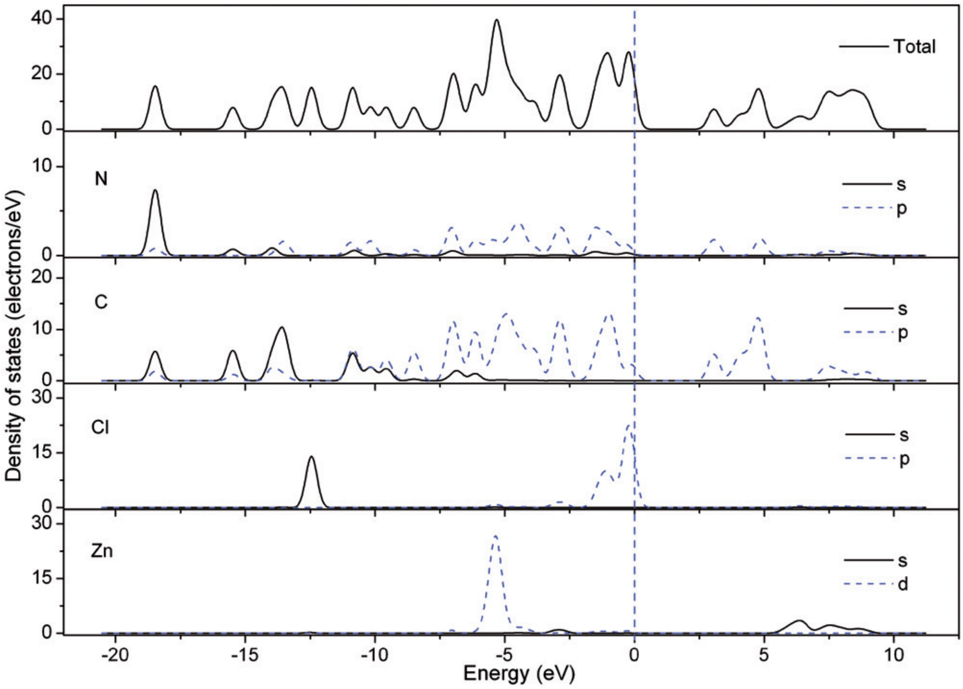

Figure 7. Total and partial DOSs of **1**. The Fermi level is set at 0 eV.

Supplementary material

CCDC-825697, 825698, 825699, 825700, 825701, and 825702 contain the supplementary crystallographic data for **1**–**6**, respectively. These data can be obtained free of charge at www.ccdc.cam.ac.uk/conts/retrieving.html (or from the Cambridge Crystallographic Data Centre, 12 Union Road, Cambridge CB2 1EZ, UK; Fax: +441223/336-033; E-mail: deposit@ccdc.cam.ac.uk).

Acknowledgments

We gratefully acknowledge the financial support of the NSF of China (20801026), the NSF of Jiangxi Province (20114BAB203005), the Aviation Science Foundation of China (2008ZF56012), Science Foundation of State Key Laboratory of Structural Chemistry (20100015), and Open Fund of the Key Laboratory of Nondestructive Testing, Ministry of Education, Nanchang Hangkong University (ZD200929007).

References

[1] M. Fujita, H. Oka, K. Yamaguchi, K. Ogura. *Nature*, **378**, 469 (1995).
[2] H.-L. Gao, L. Yi, B. Zhao, X.-Q. Zhao, P. Cheng, D.-Z. Liao, S.-P. Yan. *Inorg. Chem.*, **47**, 11057 (2008).
[3] M. Ghadermazi, F. Manteghi, H. Aghabozorg. *Acta Crystallogr., Sect. E*, **65**, 1374 (2009).

[4] J.-P. Zou, Q. Peng, G.-S. Zeng, Z.-H. Wen, Q.-J. Xing, M.-H. Chen, G.-C. Guo, J.-S. Huang. *J. Mol. Struct*., **921**, 323 (2009).

[5] G.-W. Zhou, G.-C. Guo, L.-Z. Cai, B. Liu, J.-S. Huang. *Chin. J. Struct. Chem*., **25**, 59 (2006).

[6] S.K. Ghosh, J. Ribas, M.S. El Fallah, P.K. Bharadwaj. *Inorg. Chem*., **44**, 3856 (2005).

[7] J. Soleimannejad, H. Aghabozorg, F. Manteghi, S. Najafi. *Acta Crystallogr., Sect. E*, **65**, 761 (2009).

[8] M. Devereux, M. McCann, V. Leon, V. McKee, R.J. Ball. *Polyhedron*, **21**, 1063 (2002).

[9] M. Fuijita, Y.I. Kwon, S. Washizu, K. Ogura. *J. Am. Chem. Soc*., **116**, 1551 (1994).

[10] V. Berl, I. Hue, R.G. Khoury, J.M. Lehn. *Chem. Eur. J*., **7**, 2798 (2001).

[11] T. Fessmann, J.-D. Kilburn. *Angew. Chem. Int. Ed*., **38**, 1993 (1999).

[12] Y. Nakatsuji, J.-S. Bradshaw, P.-K. Tse, G. Arena, B.-E. Wilson, N.-K. Wilson, N.-K. Dalley, R.-M. Izatt. *Chem. Commun*., 749 (1985).

[13] M. Searcey, S. MeClean, B. Madden, A.T. McGown, L.P.G. Wakelin. *Anti-Cancer Drug Des*., **13**, 837 (1998).

[14] J.-P. Zou, G.-W. Zhou, X. Zhang, M.-S. Wang, Y.-B. Lu, W.-W. Zhou, Z.-J. Zhang, G.-C. Guo, J.-S. Huang. *CrystEngComm*, **11**, 972 (2009).

[15] B. Zhao, H.-L. Gao, X.-Y. Chen, P. Cheng, W. Shi, D.-Z. Liao, S.-P. Yan, Z.-H. Jiang. *Chem. Eur. J*., **12**, 149 (2006).

[16] J.-P. Zou, G.-S. Zeng, Z.-H. Wen, Q. Peng, Q.-J. Xing, M.-H. Chen, G.-C. Guo, J.-S. Huang. *Inorg. Chim. Acta*, **362**, 4843 (2009).

[17] J.-P. Zou, Q. Peng, Z.-H. Wen, G.-S. Zeng, Q.-J. Xing, G.-C. Guo. *Cryst. Growth Des*., **10**, 2613 (2010).

[18] X. Zhao, Z. Chen, B. Zhao, W. Shi, P. Cheng. *Inorg. Chem. Commun*., **10**, 1433 (2007).

[19] J.-P. Zou, Q.-J. Xing, Z.-H. Wen, G.-S. Zeng, Q. Peng, G.-C. Guo. *Aust. J. Chem*., **63**, 942 (2010).

[20] S.K. Ghosh, S. Neogi, E.C. Sanudo, P.K. Bharadwaj. *Inorg. Chim. Acta*, **361**, 56 (2008).

[21] B. Zhao, X.-Q. Zhao, Z. Chen, W. Shi, P. Cheng, S.-P. Yan, D.-Z. Liao. *CrystEngComm*, **10**, 1144 (2008).

[22] L. Yang, A. Cour, O.P. Anderson, D.C. Crans. *Inorg. Chem*., **41**, 6322 (2002).

[23] J.-P. Zou, X.-M. Liu, L.-S. Yan, A.-M. Deng, Q.-J. Xing, M.-H. Chen. *J. Coord. Chem*., **63**, 56 (2010).

[24] J.-P. Zou, G.-W. Zhou, G.-C. Guo, L.-S. Yan, G.-S. Zeng, J.-S. Huang. *Chin. J. Struct. Chem*., **27**, 1323 (2008).

[25] G.-W. Zhou, Y.-Z. Lan, F.-K. Zheng, X. Zhang, M.-H. Lin, G.-C. Guo, J.-S. Huang. *Chem. Phys. Lett*., **426**, 341 (2006).

[26] D.C. Crans, M. Mahroof-Tahir, M.D. Johnson, P.C. Wilkins, L. Yang. *Inorg. Chim. Acta*, **356**, 365 (2003).

[27] H.-L. Gao, L. Yi, B. Zhao, X.-Q. Zhao, P. Cheng, D.-Z. Liao, S.-P. Yan. *Inorg. Chem. Commun*., **45**, 5980 (2006).

[28] J.-P. Zou, Z.-H. Wen, Q. Peng, G.-S. Zeng, Q.-J. Xing, M.-H. Chen. *J. Coord. Chem*., **62**, 3324 (2009).

[29] S.W. Ng. *Z. Kristallogr*., **213**, 421 (1998).

[30] J.-P. Zou, S.-L. Luo, M.-J. Li, X.-H. Tang, Q.-J. Xing, Q. Peng, G.-C. Guo. *Polyhedron*, **29**, 2674 (2010).

[31] J.-P. Zou, M.-H. Chen, S.-L. Luo, X.-H. Tang, Z.-Q. Xiong, Q. Peng. *Inorg. Chim. Acta*, **373**, 243 (2011).

[32] J.-P. Zou, M.-H. Chen, M.-J. Li, Q.-J. Xing, A.-Q. Zhang, Q. Peng. *J. Coord. Chem*., **63**, 3576 (2010).

[33] J.-P. Zou, M.-H. Chen, L.-Z. Zhang, Q.-J. Xing, Z.-Q. Xiong. *J. Chem. Crystallogr*., **41**, 1820 (2011).

[34] *Siemens SHELXTL^{TM} Version 5 Reference Manual*, Siemens Energy & Automation Inc., Madison, WI, USA (1994).

[35] M. Segall, P. Linda, M. Probert, C. Pickard, P. Hasnip, S. Clark, M. Payne. *Materials Studio CASTEP*, (*Version* 2.2), Accelrys, San Diego, CA (2002).

[36] M. Segall, P. Linda, M. Probert, C. Pickard, P. Hasnip, S. Clark, M. Payne. *J. Phys.: Condens. Matter*, **14**, 2717 (2002).

[37] D.R. Hamann, M. Schluter, C. Chiang. *Phys. Rev. Lett*., **43**, 1494 (1979).

[38] F. Bassani, G.P. Parravicini. *Electronic States and Optical Transitions in Solids*, Pergamon Press Ltd., Oxford, p. 149 (1975).

[39] M. Yaghi, G.M. Li. *Angew. Chem. Int. Ed*., **34**, 207 (1995).

[40] J.Y. Lu, B.R. Cabrera, R.J. Wang, J. Li. *Inorg. Chem*., **38**, 4608 (1999).

[41] M.A. Lawandy, X.Y. Huang, R.J. Wang, J. Li, J.Y. Lu. *Inorg. Chem*., **38**, 5410 (1999).

[42] J.R. Ferraro, K.C. Davis. *Inorg. Chim. Acta*, **3**, 685 (1969).

[43] H. Aghabozorg, S. Saadaty, E. Motyeian, M. Ghadermazi, F. Manteghi. *Acta Crystallogr., Sect. E*, **64**, 466 (2008).

[44] Y.-Z. Tang, Y.-H. Tan, S.-H. Chen, Y.-W. Chao. *Z. Anorg. Allg. Chem*., **633**, 332 (2007).

[45] H.-L. Gao, L. Yi, B. Zhao, X.-Q. Zhao, P. Cheng, D.-Z. Liao, S.-P. Yan. *Inorg. Chem*., **45**, 5980 (2006).

[46] S.K. Ghosh, J. Ribas, M.S. El Fallah, P.K. Bharadwaj. *Inorg. Chem*., **44**, 3856 (2005).

[47] M. Devereux, M. McCann, V. Leon, V. McKee, R.J. Ball. *Polyhedron*, **21**, 1063 (2002).

[48] H. Eshtiagh-Hosseini, M. Mirzaei, Z. Yousefi, H. Puschmann, A. Shokrollahi, R. Aghaei. *J. Coord. Chem*., **64**, 3969 (2011).

[49] Y.-Q. Yang, C.-H. Li, W. Li, Z.-J. Yi. *Chin. J. Inorg. Chem*., **25**, 1304 (2009).